TOLERANCE STUDIES OF THE MAX-IV LINAC

P. H. Williams*, D. Angal-Kalinin & J. K. Jones, STFC Daresbury Lab. & Cockcroft Inst., UK
S. Thorin, M. Eriksson & S. Werin, MaxLab, Sweden

Abstract

The MAX-IV linac will be used for both injection and top-up into two storage rings, and as a high brightness injector for a Short Pulse Facility with the option to upgrade to a Free Electron Laser in future. We briefly describe the layout, optics and bunch compression / linearisation scheme of the linac. We then investigate the robustness of the design to element errors.

INTRODUCTION

The Max-IV project [1] is currently under construction and consists of two storage rings, a full energy 3 GeV linac and Short Pulse Facility (SPF). The gun and linac will operate in a flexible way, providing injection and top-up to the rings and high-brightness pulses to the SPF. The SPF will then produce sub-ps x-ray pulses through spontaneous undulator radiation. In phase two of the project an additional beamline containing a Free Electron Laser (FEL) will be added [2], the gun, linac and beam transport must thus be capable of providing low emittance pulses to drive the FEL in future. To this end, detailed simulations including tolerance and jitter studies of the gun have been performed [3].

LINAC LAYOUT & OPTICS

Figure 1 shows the schematic layout of the linac. Compression and linearisation are performed using two double achromats with positive first order momentum compaction, R_{56}. The natural second order momentum compaction, T_{566}, from the achromats is used together with weak sextupoles to linearise the longitudinal phase space. The design thus requires no linearising harmonic cavity. The optics within the linac uses only six quadrupoles in 200 m. This restrictive use of focusing elements leads to a simple and cost effective design, however it opens up a potential sensitivity to misalignments and transverse wakefields. For further details on the achromat design and tracking studies, the reader is referred to [4].

MAGNET TOLERANCE STUDIES

In this paper, we consider in detail the sensitivity of the baseline design to errors in the magnetic elements. The errors assessed were position, orientation, field strength and multipole components. For each error, two classes of study were undertaken: individual magnet sensitivity; and the effect of Gaussian distributed random errors on all magnets. The parameters used in assessing sensitivity are predominantly percentage change in bunch length, but also projected and slice horizontal emittance where these are significantly changed. Practically, parallel ELEGANT [5] is interfaced to Mathematica and perturbed machine lattices generated automatically, typically many hundreds per individual study. The baseline bunch distribution is then tracked through each machine using North-West Grid Infrastructure parallel computing clusters. The effects of longitudinal and transverse wakefields from the linac structure, coherent and incoherent synchrotron radiation and longitudinal space charge are taken into account in all cases. Final bunch properties are then collated and analysed.

Baseline Final Bunch Properties

We tune the Max-IV linac in SPF mode, Fig. 2 shows the final bunch properties. The beam energy is 3.1 GeV, with peak current of 12 kA (a bunch length of 20 fs FWHM). Slice normalised horizontal emittance in the region of the peak current is degraded to 0.7 mm mrad, and slice energy spread at that point is 0.12%.

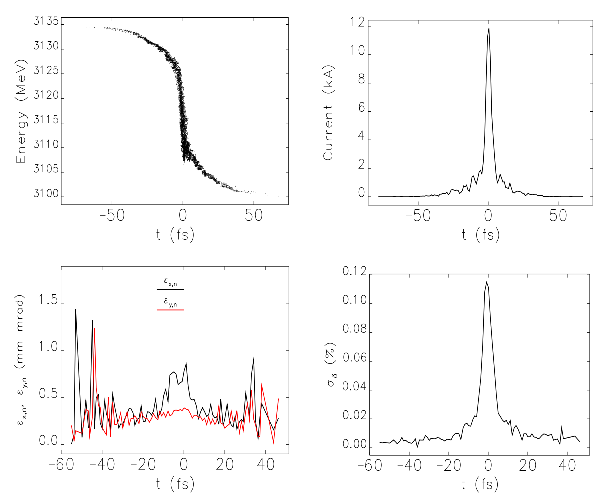

Figure 2: Baseline (SPF) final bunch properties: (1) longitudinal phase space, (2) current profile, (3) slice emittances & (4) slice energy spread.

Individual Element Tolerances

We now vary a parameter of every individual element in turn in order to assess the sensitivity of the machine tuning to each element. This will allow us to identify those components requiring more stringent specifications

* peter.williams@stfc.ac.uk

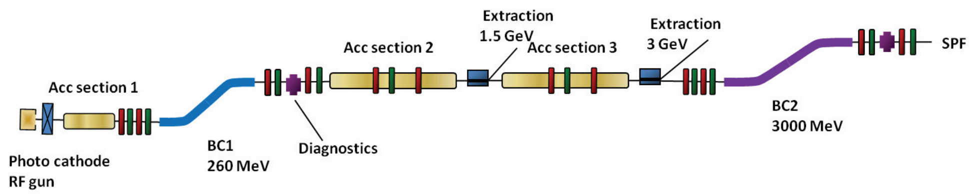

Figure 1: Layout of the Max-IV linac.

Table 1: Glossary of Machine Element Positions

Type	Group Label	Position
Quad	LINQ	before acc section 1
Quad	MATCH1Q	after acc section 1
Quad	QM	disp. sections of BC1
Quad	QFEND, QDEND	non-disp. secns. BC1
Quad	MATCH2Q	after BC1
Quad	MAINQ	within acc secns. 2/3
Quad	PREBC2Q	before BC2
Quad	QM2	disp. sections of BC2
Quad	QFEND2, QDEND2	non-disp. secns. BC2
Quad	Q21, Q22, BC2BQ	non-disp. secns. BC2
Dipole	H1, H2	BC1
Dipole	H12, H22	BC2
Sext.	S1, S2	BC1
Sext.	S12, S22	BC2

and scrutiny during machine commissioning. Specifically, for quadrupoles we vary field strength at 0.5% and 0.05% (Fig. 3), horizontal and vertical position offsets by $10\ \mu$m (Fig. 4), roll about beamline axis by $10\ \mu$rad and a selection of multipole components (skew sextupole at 0.05%, normal 12-pole (Fig. 5) and 20-pole allowed harmonics at 0.5%, and normal sextupole disallowed harmonic at 0.05%). For dipoles, we vary field strength at 0.05% and roll about the beamline axis by $10\ \mu$rad (Fig. 6). For sextupoles, we vary field strength at 0.5% (Fig. 7) and roll about the beamline axis by $10\ \mu$rad. Table 1 provides a description of where individual elements are located in the machine. Note, we do not show the results of all studies undertaken due to space restrictions.

Gaussian Distributed Error Tolerances

We now study the effect of applying Gaussian distributed random errors to the parameters of all quadrupoles. This will allow us to estimate the likely effect of a specified tolerance level on the final bunch properties. Specifically, we apply Gaussian distributed ramdom errors in field strength with standard deviations of 1×10^{-5}, 10×10^{-5} and 50×10^{-5}, and in horizontal position with standard deviations of 100 nm, $1\ \mu$m and $10\ \mu$m. For each set, we generate 50 machines and track through each one. Final bunch properties are calculated for each and an RMS in the

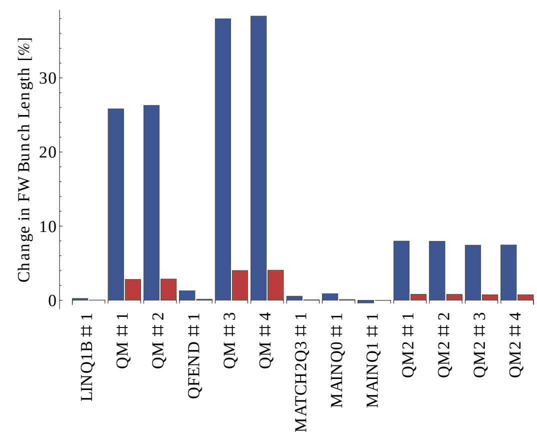

Figure 3: Change in FW bunch length from nominal on variation of quadrupole field strength by $+0.5\%$ (blue) and $+0.05\%$ (red). Only machines where change $\geq\ 0.02\%$ shown. The largest 8 are within the two bunch compressors (with BC1 dominating).

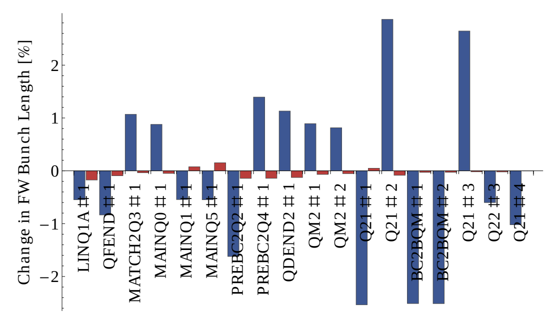

Figure 4: Change in FW bunch length from nominal on displacement in horizontal position (blue) and vertical position (green) of quadrupole by $+10\ \mu$m. Only machines where change $\geq\ 0.5\%$ shown. Unlike Fig. 3 we see that the most sensitive components are at high energy in BC2.

indicative parameter calculated. Figure 8 shows the results for field strength errors.

CONCLUSIONS

From the individual element study we conclude that the quadrupoles within dispersive sections of the bunch compressors are most sensitive. We shall mitigate this by specifying more stringent tolerances on these during manufac-

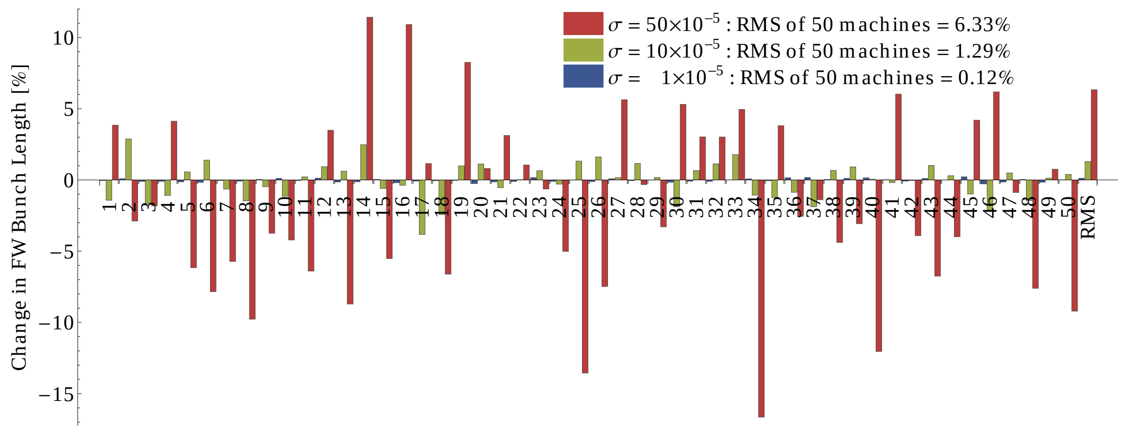

Figure 8: Change in FW bunch length for three sets of 50 machines with Gaussian distributed errors in quadrupole field strength with standard deviation shown. We see that the derived RMS of the 50 machines (final column) rises linearly with the standard deviation of the errors.

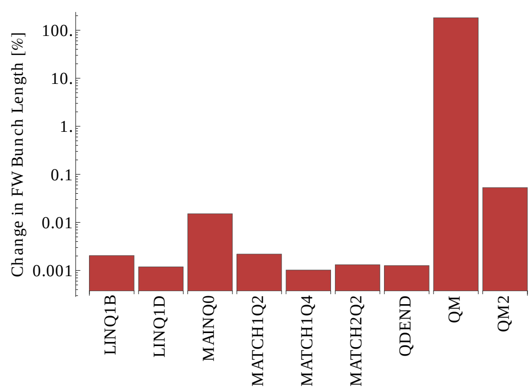

Figure 5: Change in FW bunch length on addition of $+0.5\%$ normal 12-pole field error to labelled quadrupole. Only machines where change $\geq 0.001\%$ shown.

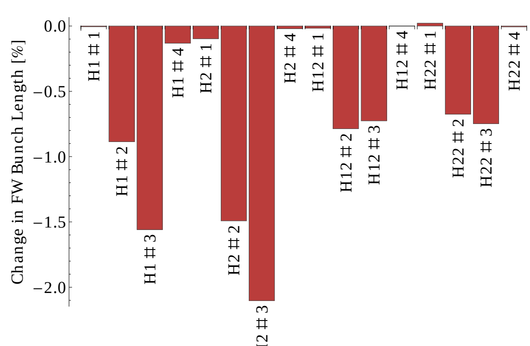

Figure 6: Change in FW bunch length under a 10 μrad dipole roll. Each dipole is treated independently.

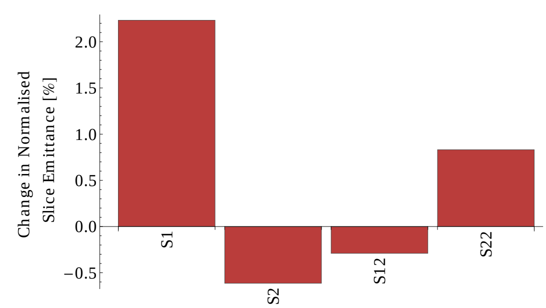

Figure 7: Change in normalised slice emittance at peak current slice from nominal on variation of sextupole field strength by $+0.5\%$.

ture, machine construction and commissioning. From the Gaussian distributed error study, we expect to be able to achieve the nominal bunch length to within 1% if we specify an error on field strength with std. dev. of 10×10^{-5} and on horizontal position of 1 μm.

The authors wish to thank Rob Allan and Tim Franks of the Computational Science Department at Daresbury Laboratory, and Jonathan Smith of Tech-X UK Ltd. for computational support.

REFERENCES

[1] Max-IV Detailed Design Report (2010), available at http://www.maxlab.lu.se/maxlab/max4/DDR_public/.

[2] S. Werin et. al., Nuclear Instruments & Methods in Physics Research A 601 (2009) 98-107.

[3] J. W. McKenzie et. al., THPC131, these proceedings.

[4] S. Thorin et. al., THPC125, these proceedings.

[5] M. Borland, Advanced Photon Source, LS-287 (2000).